International Journal of Thermophysics, Vol. 9, No. 5, 1988

Equilibrium and Transport Properties of Mixed Electrolytes[1]

E. C. Zhong[2] and H. L. Friedman[2]

The mixing rules which govern the changes in thermodynamic properties when electrolytes are mixed are briefly reviewed. Similar rules have been reported on the basis of both experiments and model calculations to govern the change in electrical conductivity when electrolytes are mixed. New model calculations show that there also is a Cassel–Wood effect in the conductivity of mixtures of electrolytes of different charge types.

KEY WORDS: electrical conductivity; electrolytes; mixtures; solutions; thermodynamic properties; transport properties.

1. INTRODUCTION

Mixed electrolyte solutions have presented many problems concerning how best to represent the mixture properties and relate them to the constituent single electrolytes [1, 2]. In any mixture there are pair interactions that are not present in the single electrolytes, so the mixtures constitute a source of information [3–5] about the new pairwise interactions. On the other hand, it transpires that the specific interaction within sets of three or more ions contribute so little that the properties of many mixtures of three or more electrolytes over a wide range of compositions can be predicted quite well from the properties of single electrolytes and binary mixtures thereof [5].

To focus on the interactions that are "turned on" when the mixture is formed, we write, for a chosen measurable property P, its change on mixing at fixed temperature, pressure, and ionic strength I,

$$\Delta_m P(y, I) \equiv P(y, I) - yP(1, I) - (1 - y)\, P(0, I) \tag{1}$$

[1] Invited paper presented at the Tenth Symposium on Thermophysical Properties, June 20–23, 1988, Gaithersburg, Maryland, U.S.A.

[2] Department of Chemistry, State University of New York, Stony Brook, New York 11794-3400, U.S.A.

0195-928X/88/0900-0677$06.00/0

where y is the fraction of the ionic strength due to one of the electrolytes and P is the amount of a chosen extensive variable per unit amount of solution.

For example, P may be $(RT)^{-1}$ times the excess free energy G^{ex} per amount of solution containing 1 kg of solvent; then I is most naturally the molal ionic strength $\frac{1}{2}\Sigma_s m_s z_s^2$, where z_s is the electrovalence and m_s is the molality of species s (see Appendix A). Other thermodynamic mixing functions can be obtained by thermodynamic differentiation of $\Delta_m G^{ex}(y, I)$. Some aspects of this relatively well-known part of the study of electrolyte mixtures are discussed in Section 2.

In the other cases reported here P is 1000 times the specific conductivity [1, 2] σ of the electrolyte solution. The systematic investigation of mixing effects on transport properties has begun, whether experimentally or theoretically, only very recently [6, 7].

2. THERMODYNAMIC PROPERTIES

The theoretical basis for the study of mixtures of electrolytes at equilibrium is the cluster expansion for the free energy of an ionic solution of arbitrary composition. Thus the excess Helmholtz free energy of a volume V of solution is given by

$$-\beta A^{ex}/V = \kappa^3/12\pi + \Sigma_{ab}\rho_a\rho_b B_{ab}(\kappa) + \Sigma_{abc}\rho_a\rho_b\rho_c B_{abc}(\kappa) + \cdots \quad (2)$$

where $\beta = 1/k_B T$, ρ_a is the particle number density of species a (at a certain elevated pressure [3, 8, 9]; Appendix A), and $B_{ab\ldots}(\kappa)$ is a modified cluster integral on a set of ions of the indicated composition. The modification involves the Mayer [10] rearrangement (renormalization) in which chains of Coulomb $1/r$ interactions are summed to give $e^{-\kappa r}/r$. The theory of electrolyte mixtures folows from the fact that, when the mixing operator Δ_m of Eq. (1) is aplied to Eq. (2), only the explicit concentration factors ρ_a, ρ_b,..., change, the cluster integrals being merely constant coefficients [3]. If we write

$$\Gamma_m P(y, I) = I^2 y(1-y)[p_0(I) + (1-2y)p_1(I) + (1-2y)^2 p_2(I) + \cdots] \quad (3)$$

then the coefficients $p_n(I)$ (which are independent of y) are linear combinations of the modified cluster integrals $B_{ab\ldots}(\kappa)$. The *secular* I dependence of $p_n(I)$ is I^n; it would be the actual I dependence except for the long range of the Coulombic and hydrodynamic interactions. As a consequence of the Mayer rearrangement, the modified cluster integrals, which may be written as functionals of $e^{-\kappa r}$, diverge mostly [11] as $\kappa \to 0$.

Each electrolyte mixing rule originally was formulated for some thermodynamic derivative of G^{ex}, but we formulate them in terms of G^{ex}

itself, thus with $P = G^{ex}/RTW$, where G^{ex} is the extensive excess Gibbs free energy and W is the number of kilograms of solvent.

The first is Harned's rule (also called Young's rule), according to which the p_0 term in Eq. (3) dominates the rest; the experimental data are adequately represented by Eq. (3) truncated after the p_0 term.

The second is the cross-square rule ($\times\,\square$ rule; also called Young's cross-square rule). To define it we introduce the four electrolytes E_{13}, E_{23}, E_{14}, and E_{24} that may be formed from cations of species 1 and 2 and anions of species 3 and 4. From these electrolytes one can form four common-ion mixtures $E_{13}+E_{13}$, etc., and two cross mixtures, $E_{13}+E_{24}$ and $E_{23}+E_{14}$, all with the same ionic strength I; then the sum of the four $\Delta_m P(\frac{1}{2}, I)$ for the common-ion mixtures is denoted $\Sigma\square$, while the sum of the other two $\Delta_m P(\frac{1}{2}, I)$ is denoted $\Sigma\times$. The simple $\times\,\square$ rule we use is $\Sigma\times = \Sigma\square$. In Appendix B other cross-square rules [12, 13] are given. Often it is found that Harned's rule and the $\times\,\square$ rule are realistic in a wide concentration range from, say, 0.5 to 5 molal ionic strength.

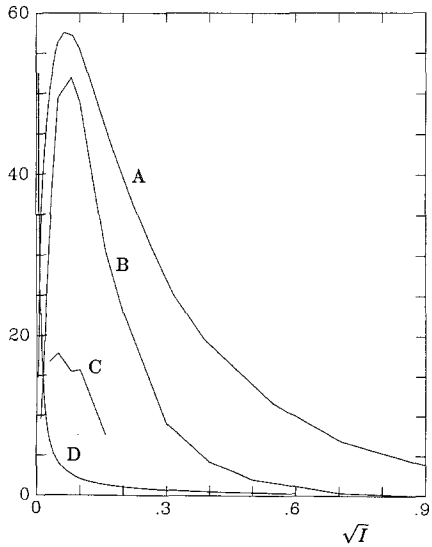

Fig. 1. Mixing coefficients $P_1(I)$ for a model for aqueous LiCl, $MnCl_2$ mixtures. A is the free energy function $4000g_1(I)$, with $g_1(I)$ taken from Ref. 14. The scale factor is merely to facilitate visual comparison with σ_1. B is $\sigma_1(I)$ calculated for the same model. The calculation for C is the same as for B, except that the model Mn^{2+}, Cl^- Gurney parameter [14, 18] has been increased by $0.1k_BT$. D is an additive contribution to $\sigma_1(I)$ from $S(y)$, as described in the text.

Now we turn to a third regularity which concerns the behavior of the $p_1(I)$ coefficient in very dilute mixtures of two electrolytes of different charge types, the Cassel–Wood effect [15]. When the ionic charges z_1 and z_2 are not the same, then for a mixture $E_{13}+E_{23}$ the *limiting law* $p_1(I) \to CI^{1/2}$ holds at sufficiently small I, with a coefficient C that depends on the ions only through their charges [14–16]. Cassel and Wood [15] measured enthalpies of mixing for two such unsymmetrical mixtures. With $P = H/RTW$, where H is the extensive enthalpy, they found that $p_1(I)$ is very small in the molar concentration range, but in the range from $I = 1$ to $I = 0.01$ the coefficient $p_1(I)$ increases strongly as I is *lowered.* Thus, in viw of the limiting law for p_1, a peak in $p_1(I)$ at very low concentrations was predicted [16] and actually located (under the HNC approximation) for a modal for a mixture of LiCl and $McCl_2$ [14]. The latter calculation locates the peak near $I = 10^{-3}$ m (see Fig. 1), too dilute for the required thermodynamic properties to be measured by known methods.

3. TRANSPORT IN MIXED ELECTROLYTES

Historically the electrical conductivity of ionic solutions has been the most important property for investigating them, so it is interesting to ask what we may learn about electrolyte mixtures from conductivity data. In this endeavor we use a cluster expansion for the conductivity of electrolytes [17] together with an approximation method of the integral equation type [18] that can be applied to solution models to calculate the conductivity as well as the ionic self and distinct diffusion coefficients. The distinct diffusion coefficient D^{d}_{ab} is especially interesting because it vanishes in the absense of interactions between the a ion and the n ion, so it is a remarkably direct measure of the pair interaction [18]. However, here the only transport property we discuss is the specific conductivity σ. We note that, in the physical chemistry of solutions of single electrolytes, σ is usually addressed in the combination $\Lambda = 100\sigma/N$, where Λ is the *equivalent conductivity* and N is the *normality* (equivalents per liter). Because of our fixation with mixing at a constant ionic strength (Section 2), we would replace the equivalent conductivity by the *ionic strength conductivity* $\Lambda' = 1000\sigma/I$ Appendix A).

Now we ask whether we expect to find that Harned's rule and the $\times \square$ rule are valid when $P(y, I) = 1000[\sigma(y, I)]$. An answer is found by beginning with a cluster expansion [17] that is analogous to Eq. (2). We recall that in the latter the term $-\kappa^3/12\pi$ derives from the sum over all ring graphs made by closing chains of Coulomb bonds $[-\beta u^{C}_{ab}(r)$ bond $= -\beta e_a e_b/\varepsilon r]$ on black ρ_{ion} vertices. Of course in Eq. (2) the κ

dependence of the cluster integrals derives from the sum of such Coulomb-bond, ρ-vertex chains. The cluster expansion of the conductivity is

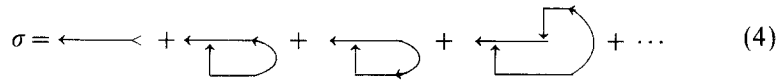

(4)

where the first term on the right is the ideal conductivity. In these diagrams the secular I dependence is L^n, where n is the number of horizontal lines, one for each ion in the cluster. The actual I dependence is weaker than the secular because the *static* chain sums [also involved in Eq. (2)] given divergent contributions to the integrals as $\kappa \to 0$. In addition, there are *dynamical* chain sums, as we shall see. They are not constant for variations in composition at fixed I. [While analyzing Eq. (4) to a degree that is sufficient to explain the role of the dynamical chain sums, we refer to an earlier report for many aspects that are omitted here (Ref. 17, Fig. 1).] In each diagram time increases from right to left. The curved lines represent equilibrium spatial correlations $g_{ab}(r)-1$ at $t=0$, which are adequately approximated here by $-\beta u_{ab}^{C}(r)e^{-\kappa r}$. The Debye shielding factor $e^{-\kappa r}$ xomes from the Mayer rearrangement that is used to generate the static chain sums in the modified cluster integrals in Eq. (2); the contribution of $g_{ab}(r)$ is a *static* effect; it does not depend on the mobilities of the ions.

The vertical straight lines represent forces between ions; the longest ranged are $-\vec{\nabla}u_{ab}^{C}(r)$ and hydrodynamic forces. These interactions all contribute to the asymptotic dependence of σ on I as $I \to 0$. More generally, however, the non-Coulombic part of the pair interactions must be included, as well as more tightly connected diagrams (i.e., with multiple vertical lines that collectively represent nonlinear interactions.

The horizontal lines in Eq. (4) are ion propagators, self-van Hove functions in phase space. In certain limiting cases the propagator for an a ion reduces to

$$\exp\{-[r(t)-r(0)]^2/4D_a^{s0}t\}/(4\pi D_a^{s0}t)^{1/2}$$

which illustrates the role of the *bare* self-diffusion coefficient D_a^{s0} ($1/\beta D_a^{s0}$ is the friction coefficient) of an ion of species a in the pure solvent.

Even in the $I \to 0$ asymptotic regime the series in Eq. (4) must be extended to include the diagrams which are related to those shown by replacing the propagator-force interaction by chains of propagator-foce interactions.

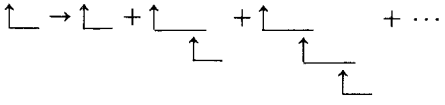

(5)

The reason for this renormalization (which gives the dynamic screening) is the usual one; taken one by one the individual terms give divergent integrals that contribute to σ, while the divergences mutually cancel when these dynamic chain sums are formed. But we must remark on some unusual features of this renormalization. One is that the lowest-order terms are not divergent; each cluster diagram in Eq. (4) represents a finite contribution to σ. But the higher terms, taken one by one, do given divergent integrals. Another is that renormalizing the diagrams in Eq. (4) has the efect on σ that Onsager ascribed to including "the Brownian motion of the ions" in his correction [19] to the Debye–Hueckel conductivity theory [20]. Finally, a typical dynamical chain sum can be reduced to [17]

$$\Sigma_b \kappa_b^2 D_b^{s0}/(D_b^{s0} + D_a^{s0}) \equiv s_a \kappa^2 \tag{6}$$

which ranges from $\frac{1}{2}\kappa^2$ (all S_a^{s0} the same) to κ^2 (one D_a^{s0} much larger than any of the others).

The most important feature of the dynamical chain sums in the context of the mixing rules is that d_a will change with composition even at fixed ionic strength unless all of the bare self-diffusion coefficients are the same. To see the consequences, we rewrite Eq. (4) in terms of the secular concentration factors in analogy to Eq. (2)

$$\sigma = \Sigma_a \rho_a C_a + \Sigma_{ab} \rho_a \rho_b C_{ab} + \Sigma_{abc} \rho_a \rho_b \rho_c C_{abc} + \cdots \tag{7}$$

where (except for the ideal term C_a) the C coefficients will vary with composition even at fixed I due to the dynamical chain sums. On this basis it would appear that the theoretical basis of the mixing rules does not extend to the case in which P is the conductivity.

To see how the composition dependence of the dynamical shielding affects the validity of the $\times \square$ rule we first test this rule in the limiting law region where the exact conductivity theory is known and where short-range specific ion–ion interactions can be neglected. To make a connection with a widely used form [21] for the concentration dependence of conductance, we write (see Appendix A)

$$\Lambda'(y, I) = \Lambda_0'(y) - S(y)\sqrt{I} + E(y) I \ln I + J(y) I + \cdots \tag{8}$$

where Λ_0' is the ideal term; it makes no contribution to $\Sigma \square$ or $\Sigma \times$. The limiting law coefficient S for an ionic solution of general composition can be expressed in terms of algebraic combinations of the ionic strength fractions, charges, and bare self-diffusion coefficients [22]. Thus in the limiting law region, the regime in which the E, J, and higher terms in Eq. (8) are negligible compared to the $S\sqrt{I}$ term, we can calculate exactly the deviation from the $\times \square$ rule for Λ' or σ.

Some typical results are reported in Table I. As expected the relative deviation

$$r_{\times\square} = (\Sigma\times - \Sigma\square)/\Sigma\square \tag{9}$$

from the $\times\square$ rule is smallest for models in which the mobilities are all the same. What was not anticipated is that, even with bare self-diffusion coefficients spread over a wide range, $|r_{\times\square}|$ is, at most, only about 1%. This is less than the experimental uncertainty in many cases, even in the molar concentration range.

It is traditional to reduce electrolyte conductivity data to equivalent conductivities on equivalent concentration (normality) scales, so we have also tested the $\times\square$ rule for mixings at constant normality (Table I). The deviations again are small.

On the basis of the results in Table I there is no apparent reason why the $\times\square$ rule for conductivity should not also be realistic at higher concentrations. Indeed this is demonstrated by the experimental tests of this rule for the conductivity of $I=\frac{1}{2}m$ mixtures of the ions K^+, Mg^{2+}, Cl^-, and NO_3^- and mixtures of K^+, Li^+, Cl^-, and SO_4^{2-} [7] and by model calculations [7] leading to Table II. Aside from the good compliance with the $\times\square$ rule, these data show only that there is scope for improvement in the models, judging by comparison with experimental data [18]. In view of the observation [5] that ion pairing causes deviations from the $\times\square$ rule, we point out that the last set of data in Table II were calculated for models in which there is a strong tendency to form Cl^-, Cl^- associated pairs [18, 25].

Table I. $\times\square$ Rule for Conductivity in the Limiting Law Regime for Mixtures with Various Charge Types and Ion Mobilities

z_i, i				$\lambda_i^0/\lvert z_i\rvert$,[a] $i=$				$1000r_{\times\square}$	
1	2	3	4	1	2	3	4	I[b]	N[c]
1	−1	1	−1	50	76	74	71	0.08	0.008
1	−1	1	−2	37	76	76	40	−12.	−1.5
1	−10	1	−10	10	10	100	100	0.4	0.5
1	−1	3	−2	350	76	20	40	−21.	8.
1	−3	2	−4	100	33	50	25	2.4	15.
1	−3	2	−4	50	50	50	50	−0.002	7.9

[a] λ_i^0 is the limiting equivallent conductivity of ion i in water at 25°C.
[b] For mixing at a constant ionic strength.
[c] For mixing at a constant normality.

Table II. × □ Rule Model Calculations: Aqueous Electrolytes at 25°C[a]

				Σ×	Σ□
NaCl[b]	−4.86	NaBr	−226		
−134.9		−131.8			
KCl	−3.90	KBr	−49.6	275.6	275.5
KCl[b]	−10.2	KNO_3	−337		
−680		−593			
$MgCl_2$	−13.8	$Mg(NO_3)_2$	−963	−1300	−1297
LiCl[b]	−47.3	Li_2SO_4	−30.6		
−331		−272			
KCl	24.3	K_2SO_4	−642	−630	−610
LiCl[c]	−360	Li_2SO_4	−8970		
−2590		−6360			
KCl	1680	K_2SO^4	630	−8340	−7630

[a] $1000\Delta_m\sigma(\frac{1}{2}, I)$ for indicated mixings. The numbers in between two electrolyte formulas pertain to mixing that pair. The numbers to the right of the "square" each pertain to the nearest cross mixing. For example, the number next to $Mg(NO_3)_2$ is for the $Mg(NO_3)_2$–KCl mixing.

[b] Calculated for charged soft-sphere models [7] at $I = 1M$.

[c] Calculated for models based on Pettitt–Rossky solvent-averaged pair potentials at $I = \frac{1}{2}M$ [25]. See footnote 25 in Ref. 7.

It might seem appropriate next to develop models that fit the experimental × □ rule data. But first we need to know more about ion–ion pair potential models that are consistent with the results of *ab initio* calculations and with the experimental excess free energies for all of the relevant single and mixed electrolytes.

Among the experimental data that would be very useful for this purpose is $g_1(I)$ [defined as the p_1 coefficient of Eq. (3) when $P = G^{ex}/RTW$] for each of the unsymmetrical common-ion mixtures. Figure 1 shows $g_1(I)$ calculated [14] from a model for aqueous mixtures of LiCl and $MnCl_2$. It turns out that the peak in $g_1(I)$, itself a remarkable feature at such low concentrations (near 10^{-3} M), is very sensitive to small changes in the model Mn^{2+}–Cl^- pair potential. In Fig. 7 of Ref. 14 this sensitivity is illustrated by claculations of certain ion–ion pair correlation functions at compositions near $I = 0.005m$; they change markedly when the model Mn^{2+}, Cl^- pair potential is made slightly less attractive by increasing the Gurney parameter $A_{Mn,Cl}$ by $0.1k_BT$ [14]. This slight change in the model lowers the peak in $g_1(I)$ from 0.014 (Fig. 1) to 0.012, so it is clear that experimental data for $g_1(I)$ would be useful for selecting or tuning the solution models of interest. Unfortunately such measurements, whether for

g_1 or any of its thermodynamic derivatives, seem to be beyond the present state of the art. However, if the corresponding efect exists in the conductivity data it might well be accessible to experimental investigation.

Therefore we have calculated the conductivity of the same LiCl, $McCl_2$ model [14, 16] to see whether the extension of the mixing rules from thermodynamics to conductivity, as has been indicated by Harned's rule and the $\times \square$ rule, also covers the Cassel–Wood effect.

The remarkable result is shown in Fig. 1 for the conductivity function $\sigma_1(I)$ which appears in the notation of Eq. (3), specialized for the case in which $P = 1009\sigma$.

$$1000\Delta_m\sigma = I^2y(1-y)[\sigma_0(I) + (1-2y)\,\sigma_1(I) + \cdots] \tag{10}$$

If the Gurney parameter for the model Mn^{2+}, Cl^- interaction is increased by $0.1k_BT$, the σ_1 curve shifts from B to C. Therefore it looks as though data for the $\sigma_1(I)$ would indeed be useful for testing and tuning model pair potential functions.

A molecular picture has been proposed for the Cassel–Wood effect in thermodynamics [14]. It involves the pair correlation functions $g_{ij}(r)$ for Li^+, Mn^{2+} pairs and Mn^{2+}, Mn^{2+} pairs and how they are affected by the formation of a weak Mn^{2+}, Cl^- ion pair complex. The effect of these interactions evidently is to lower $g_1(I)$ relative to the limiting law line and we find here a qualitatively similar change for $\sigma_1(I)$. In particular, the peaks in g_1 and σ_1 are both lowered when we make the Mn^{2+}, Cl^- interaction slightly less attractive.

Curve D in Fig. 1 represents a small but interesting complication. This has to do with the y dependence of $S(y)$ [Eq. (8)]. It makes a contribution to $\sigma_1(I)$ that diverges at $I = 0$, a feature that has no counterpart in $g_1(I)$; for thermodynamic properties the coefficient that corresponds to S has no y dependence. This in turn follows because the cluster integrals $B_{a\ldots}(\kappa)$ have no y dependence. The y dependence of $S(y)$ is an expression of the contribution of the dynamical chain sum in Eq. (6). As shown by the D curve in Fig. 1, it becomes important only at concentrations below which we have obtained accurate solutions of the integral equation theory of conductivity from which curves B and C have been calculated. Here we have another example, but entirely different from the $\times \square$ rule data, of the fact that the degree to which the dynamical chain sums differ from the equilibrium chain sums is of little importance for electrolyte mixtures.

4. CONCLUSIONS

To the degree that the AZF conductivity theory [18] is adequate for the applications developed here, we have established that the $\times \square$ rule and

the Cassel–Wood effect, both known from studies of the thermodynamics of mixed electrolytes, extend to the electrical conductivity. These results indicate that the excess conductivity is due mainly to the specific interactions of pairs of ions and ion triples, with negligible contributions from the specific interactions of larger clusters of ions. On this basis it is expected that Pitzer's equations for the thermodynamic properties of electrolyte solutions [12, 13] could be extended to the conductivity. Also, because of the great accuracy with which electrical conductivity can be measured, it may be feasible to tst for the predicted peak in $\sigma_1(I)$ in real solutions in a way that does not seem possible for $g_1(I)$ or its thermodynamic derivatives.

APPENDIX A. CONCENTRATION SCALES

In this report a number of technical details have been suppressed in order to avoid obscuring the main points. A typical aspect of this kind is the distinction between McMillan–Mayer states (MM states; where the independent variables are the chemical potential of the solvent, the temperature, and the number densities of the ions, and the convenient thermodynamic potential is the Helmholtz free energy) and Lewis–Randall states (LR states; where the independent variables are the pressure, the temperature, and the molal concentrations of the ions and the convenient thermodynamic potential is the Gibbs free energy). For thermodynamics the theory often is developed most easily for MM states, while the experimental aspects are more conveniently reported for LR states. The way to calculate one from the other, given sufficient thermodynamic data for the solutions, is well known [3, 8, 9, 23, 24]. A simple example is

$$I = \tfrac{1}{2}\Sigma_a m_a z_a^2 = \alpha\kappa^2 = \alpha 4\pi(e^2\beta/\varepsilon)\,\Sigma_a \rho_a z_a^2 \tag{11}$$

where the conversion factor α derives from the difference between the LR molalities on the left and the MM particle number densities on the right. The neglect of the concentration dependence of α in this report is typical of the technical details that are suppressed. Such approximations do not cause significant errors here. More detail would be needed for applications to systems in which the partial molar volumes of the ions are relatively large, say, for tetrabutyl ammonium ions.

APPENDIX B. VARIANTS OF THE $\times\,\square$ RULE

We introduce the notation $D(\mathrm{ca}, \mathrm{CA}) = \Delta_m P(\frac{1}{2}, I)$ for mixing E_{ca} with E_{CA}, and we write a generalized $\times\,\square$ rule

$$\Sigma \times w(\mathrm{ca}, \mathrm{CA})\, D(\mathrm{ca}, \mathrm{CA}) = \Sigma \square w(\mathrm{ca}, \mathrm{CA})\, D(\mathrm{ca}, \mathrm{CA}) \tag{12}$$

or, in more detailed form,

$$\begin{aligned} & w(\mathrm{ca}, \mathrm{CA})\, D(\mathrm{ca}, \mathrm{CA}) + w(\mathrm{cA}, \mathrm{Ca})\, D(\mathrm{cA}, \mathrm{Ca}) \\ & \quad = w(\mathrm{ca}, \mathrm{cA})\, D(\mathrm{ca}, \mathrm{cA}) + w(\mathrm{cA}, \mathrm{CA})\, D(\mathrm{cA}, \mathrm{CA}) \\ & \qquad + w(\mathrm{CA}, \mathrm{Ca})\, D(\mathrm{CA}, \mathrm{Ca}) + w(\mathrm{Ca}, \mathrm{ca})\, D(\mathrm{Ca}, \mathrm{ca}) \end{aligned} \tag{13}$$

which reduces to the simple $\times \square$ rule defined in Section 2 when all of the weight functions $w(\mathrm{ca}, \mathrm{CA})$ are the same. In another case, with

$$w(\mathrm{ca}, \mathrm{CA}) = (z_c - z_a)(z_C - z_A) \tag{14}$$

Eq. (13) becomes the *canonical* $\times \square$ rule. In the spcial case $z_c = z_C$ and $z_a = z_A$, we again recoer the simple $\times \square$ rule.

The canonical $\times \square$ rule for thermodynamic properties follows *exactly* from Eq. (2) if the series is truncated after the third virial coefficient terms [26]. So it is also consistent with Pitzer's equations, which derive from a certain modified form of the cluster expansion in Eq. (2) [12, 13]. Reilly and Wood have introduced another $\times \square$ rule with $w(\mathrm{ca}, \mathrm{CA})$ coefficients different from unity, but it is not the same as the canonical $\times \square$ rule. It is found, for both thermodynamics and conductivity and for both model calculations and experiments, that the simple $\times \square$ rule exhibits nearly the same accuracy as the canonical $\times \square$ rule, with sometimes one and sometimes the other being more accurate. Since neither can be exact for real systems, in view of the neglect of higher terms in the cluster expansion and, in the case of conductivity, in view of the y dependence of the cluster integrals, and since they are about equally accurate, we give results only for the simple $\times \square$ rule in this report.

ACKNOWLEDGMENT

The support of this research by the National Science Foundation is gratefully acknowledged.

REFERENCES

1. H. S. Harned and B. B. Owen, *The Physical Chemistry of Electrolyte Solutions*, 3rd. ed. (Reinhold, New York, 1955), Chap. 14.
2. R. A. Robinson and R. H. Stokes, *Electrolyte Solutions*, 3rd ed. (Butterworth's, London, 1955).
3. H. L. Friedman, *J. Chem. Phys.* **32**:1351 (1960).
4. H. L. Friedman, *Faraday Disc. Chem. Soc.* **85**:1 (1988).
5. P. J. Reilly and R. H. Wood, *J. Phys. Chem.* **73**:4292 (1969).
6. E. O. Timmermans, *Ber. Bunsensges. Phys. Chem.* **83**:263 (1979), and references therein.

7. Y. C. Wu, W. F. Koch, E. C. Zhong, and H. L. Friedman, **92**:1692 (1988).
8. H. L. Friedman and P. J. Ramanathan, *J. Phys. Chem.* **74**:3756 (1970).
9. H. L. Friedman, *J. Solut. Chem.* **9**:525 (1980).
10. J. E. Mayer, *J. Chem. Phys.* **18**:1476 (1950).
11. H. L. Friedman, *Mol. Phys.* **2**:110, 436 (1959).
12. K. S. Pitzer, *Acc. Chem. Res.* **10**:371 (1977).
13. K. S. Pitzer and J. C. Peiper, *J. Phys. Chem.* **84**:2396 (1980).
14. T. K. Lim, E. C. Zhong, and H. L. Friedman, *J. Phys. Chem.* **90**:144 (1986).
15. R. B. Cassel and R. H. Wood, *J. Phys. Chem.* **78**:1924 (1974).
16. H. L. Friedman and C. V. Krishnan, *J. Phys. Chem.* **78**:1927 (1974).
17. H. L. Friedman, *Physica* **30**:537 (1964).
18. E. C. Zhong and H. L. Friedman, *J. Phys. Chem.* **92**:1685 (1988).
19. L. Onsager, *Physik Z.* **27**:388 (1926); **28**:277 (1927).
20. P. Debye and E. Huckel, *Physik* **24**:305 (1923).
21. R. M. Fuoss, L. Onsager, and J. F. Skinner, *J. Phys. Chem.* **69**:2581 (1965).
22. E. C. Zhong and H. L. Friedman, *J. Solut. Chem.* **16**:337 (1987).
23. H. L. Friedman, *J. Solut. Chem.* **1**:387, 413, 418 (1972).
24. J. L. Gomez-Estevej, *J. Solut. Chem.* **16**:87 (1987).
25. B. M. Pettitt and P. J. Rossky, *J. Chem. Phys.* **84**:5836 (1986).
26. E. C. Zhong and H. L. Friedman, In preparation.